

13 **Abstract**

14 Tn5-mediated transposition of double-strand DNA has been widely utilized in
15 various high-throughput sequencing applications. Here, we report that the Tn5
16 transposase is also capable of direct tagmentation of RNA/DNA hybrids *in vitro*.
17 As a proof-of-concept application, we utilized this activity to replace the
18 traditional library construction procedure of RNA sequencing, which contains
19 many laborious and time-consuming processes. Results of activity of
20 transposase assisted RNA/DNA hybrids co-tagmentation (termed “ATRAC-seq”)
21 are comparable to traditional RNA-seq methods in terms of gene number, gene
22 body coverage and gene expression analysis; at the meantime, ATRAC-seq
23 enables a one-tube library construction protocol and hence is more rapid (within
24 8 h) and convenient. We expect this tagmentation activity on RNA/DNA hybrids
25 to have broad potentials on RNA biology and chromatin research.

26 **Introduction**

27 Transposases exist in both prokaryotes and eukaryotes and catalyze the
28 movement of defined DNA elements (transposon) to another part of the
29 genome in a “cut and paste” mechanism (1-3). Taking advantage of this
30 catalytic activity, transposases are widely used in many biomedical applications:
31 for instance, an engineered, hyperactive Tn5 transposase from *E. coli* has been
32 utilized in an *in vitro* double-stranded DNA (dsDNA) tagmentation reaction to
33 achieve rapid and low-input library construction for next-generation sequencing
34 (4-9). In addition, Tn5 was also used for *in vivo* transposition of native chromatin
35 to profile open chromatin, DNA-binding proteins and nucleosome position
36 (“ATAC-seq”) (10). While Tn5 has been broadly adopted in high-throughput
37 sequencing, bioinformatic analysis and structural studies reveal that it belongs
38 to the retroviral integrase superfamily that act on not only dsDNA but also
39 RNA/DNA hybrids (for instance, RNase H). Despite the distinct substrates,
40 these proteins all share a conserved catalytic RNase H-like domain (see Figure
41 1a) (11-14). Given their structural and mechanistic similarity, we attempted to
42 ask whether or not Tn5 is able to catalyze tagmentation reactions to RNA/DNA
43 hybrids (see Figure 1b), in addition to its canonical function of dsDNA
44 transposition. In this study, we tested this hypothesis and found that indeed Tn5
45 possesses *in vitro* tagmentation activity towards both strands of RNA/DNA
46 hybrids. As a proof of concept, we apply such activity of transposase-assisted
47 RNA/DNA hybrids co-tagmentation (ATRAC-seq) to achieve rapid and low-cost

48 RNA sequencing starting from total RNA extracted from 10,000 to 100 cells. We
49 find that ATRAC-seq data are comparable to conventional RNA-seq results in
50 terms of detected gene numbers, gene expression measurement and gene
51 body coverage, at the same time it avoids many laborious and time-consuming
52 steps in traditional RNA-seq experiments. Such Tn5-assisted tagmentation of
53 RNA/DNA hybrids could have broad applications in RNA biology and chromatin
54 research.

55

56 **Results**

57 To test whether Tn5 transposase has tagmentation activity on RNA/DNA
58 hybrids, we prepared RNA/DNA duplexes by performing mRNA reverse
59 transcription. We first validated the efficiency of reverse transcription and the
60 presence of RNA/DNA duplexes using a model mRNA sequence (~1,000 nt) as
61 template (see Figure S1a). We then subjected the prepared RNA/DNA hybrids
62 from 293T mRNA to Tn5 transposome, heat-inactivated Tn5 transposome and
63 a blank control (without Tn5), respectively (see Methods). The hybrids were
64 then recovered and their length distribution was analyzed by Fragment
65 Analyzer (see Figure 1c). Comparing with the heat-inactivated Tn5 sample or
66 the blank control sample, the Tn5 transposome sample exhibited a modest but
67 clear smear signal corresponding to small fragments ranging from ~30-650
68 base-pair (bp) (the blue patches in Figure 1c). Consistent with the
69 fragmentation event, we also observed a down shift of large fragments ranging

70 from ~700-4000 bp (the orange patches in Figure 1c). In addition, the
71 fragmentation efficiency increased in a dose-dependent manner with the
72 transposome, suggesting that fragmentation of RNA/DNA hybrids is dependent
73 on Tn5 (see Figure S1b).

74

75 We next asked whether RNA/DNA hybrids are tagged by Tn5. For a canonical
76 dsDNA substrates, the staggered tagmentation of Tn5 results in a 9 bp gap
77 between the nontransferred strand and the target DNA (see Figure 1d). We
78 anticipate that a similar *in vitro* tagmentation reaction to RNA/DNA hybrids
79 generates a structure with adaptors ligated to the 5' ends of both RNA and DNA
80 strands and gaps at the 3' ends (see Figure 1e). If such a structure is present,
81 we would be able to convert it into an amplifiable DNA sequence by reverse
82 transcription from the target DNA into this gap, followed by extension synthesis
83 of the attached adaptor sequence by strand displacement (see Figure 1e). We
84 chose *Bst* 3.0 DNA polymerase, which demonstrates strong 5'→3' DNA
85 polymerase activity with either DNA or RNA templates. We then performed
86 quantitative polymerase chain reaction (qPCR) quantification for the three
87 samples. We observed that cycle threshold (Ct) value of the Tn5 transposome
88 sample is about 8 cycles smaller than the heat inactivated Tn5 sample or the
89 control sample, indicating approximately 256 times more amplifiable products
90 (see Figure 1f). We also tested different buffer conditions and found that the
91 performance of Tn5 remained similar, indicating the robustness of the Tn5

92 tagmentation activity (see Figure S1c). Using Sanger sequencing, we validated
93 that the adaptor sequences are indeed ligated to the insert sequences (see
94 Figure S1d). Therefore, Tn5 can simultaneously fragment and ligate adaptors
95 to both strands of RNA/DNA hybrids.

96

97 Having demonstrated the tagmentation activity of Tn5 on RNA/DNA hybrids, we
98 then thought about its potential application. RNA/DNA duplexes can be found
99 in many *in vivo* scenarios, including but not limited to R-loop and chromatin-
100 bound lncRNAs (15, 16). Under *in vitro* conditions, RNA/DNA hybrids are also
101 key intermediates in various molecular biology and genomics experiments. For
102 instance, RNA has to be first reverse transcribed into cDNA in a traditional RNA-
103 seq experiment so as to construct a library for sequencing. Because traditional
104 RNA-seq library construction involves many laborious and time-consuming
105 steps, including mRNA purification, fragmentation, reverse transcription,
106 second-strand synthesis, end-repair and adaptor ligation, we attempted to
107 replace the process using the tagmentation activity towards RNA/DNA
108 duplexes. With the help of ATRAC-seq, these steps are replaced with a “one-
109 tube” protocol (see Figure 2a), which uses total RNA as input material and
110 involves just three seamless steps (reverse transcription, tagmentation and
111 strand extension), without the need for a second strand synthesis step. We first
112 conducted ATRAC-seq with 200 ng total RNA as input; we observed very high
113 correlation in gene-expression levels among three replicates, indicating

114 ATRAC-seq is highly reproducible (see Figure 2b). To test the robustness of
115 ATRAC-seq, we performed the experiments with 20 ng and 2 ng total RNA.
116 ATRAC-seq results are again highly reproducible among replicates (see Figure
117 S2a, S2b). More importantly, gene expression level measured using different
118 amount of starting materials remain consistent with each other (see Figure 2c).
119
120 We then compared the library quality between ATRAC-seq and NEBNext Ultra
121 II RNA library prep kit, a commonly used kit for RNA-seq library construction.
122 We found that ATRAC-seq libraries exhibited similar percentage of reads
123 mapped to annotated transcripts, rRNA contamination and gene numbers to
124 NEBNext data (see Table S1), despite the fact that ATRAC-seq directly uses
125 total RNA as input material. Most of the genes detected by ATRAC-seq overlaps
126 with that of NEBNext, with slightly more genes detected by ATRAC-seq (see
127 Figure 2d). In addition, ATRAC-seq showed comparable performance to
128 NEBNext in terms of gene expression measurement (see Figure 2e).
129 Compared to NEBNext, the insert size of ATRAC-seq library was considerably
130 shorter (see Figure S2c); nevertheless, we observed similar coverage
131 distribution over gene body. ATRAC-seq also showed a slight tendency to 3'
132 end of the gene body (see Figure 2f). This 3' bias of gene coverage decreased
133 as the amount of starting materials reduced; hence it is likely due to incomplete
134 reverse transcription of the 5' end of transcripts when oligodT primers were
135 used. Further inspection of reads distribution of ATRAC-seq over genome

136 features revealed similar pattern for that of NEBNext (see Figure 2g).

137 Coverages of some representative transcripts are shown in Figure 2h and
138 Figure S2d.

139

140 To further investigate whether potential bias exists for ATRAC-seq, we
141 compared the GC content of library prepared by ATRAC-seq with that of
142 NEBNext. We found an enrichment of fragments with higher GC content in the
143 ATRAC-seq libraries (see Figure S2e); whether or not this is due to the
144 increased stability of GC-rich RNA/DNA hybrids, which is an asymmetric
145 intermediate between A and B forms (17), remains to be demonstrated.

146 Previous studies also found that Tn5 exhibits a slight insertion bias on dsDNA
147 substrates (18-20). We thus characterized sites of Tn5-catalyzed adaptor
148 insertion by calculating nucleotide composition of the first and last 10 bases of
149 each sequencing read after adaptor trimming. Similar to dsDNA substrates, we
150 also observed an apparent insertion signature on RNA/DNA hybrids (see Figure
151 S2f). Nevertheless, per-position information contents were extremely low,
152 suggesting such insertion bias is less likely to affect the uniformity of gene body
153 coverage (see Figure S2g). Overall, when utilized as a library preparation
154 method, ATRAC-seq demonstrates comparable performance with a traditional
155 RNA library preparation method, but outcompetes the traditional method in
156 terms of speed, convenience and cost.

157

158 **Discussion**

159 Based on substrate diversity and the conserved catalytic domain of the
160 retroviral integrase superfamily including the Tn5 transposase, we envision in
161 this study that Tn5 may be able to directly tagment RNA/DNA hybrid duplexes,
162 in addition to its canonical dsDNA substrates. Having validated such *in vitro*
163 tagmentation activity, we developed ATRAC-seq, which enables one-tube, low-
164 input and low-cost library construction for RNA-seq experiments. Compared to
165 conventional RNA-seq methods, ATRAC-seq does not need to pre-extract
166 mRNA and synthesize a second DNA chain after mRNA reverse transcription.
167 Therefore, ATRAC-seq bypasses laborious and time-consuming processes, is
168 compatible with low input, and reduces reagent cost. Collectively, these
169 features enable library construction mediated by ATRAC-seq to competes the
170 traditional methods.

171

172 Despite its unique advantages, there is room to further improve ATRAC-seq.
173 For instance, ATRAC-seq exhibits signature at sites of adaptor insertion as well
174 as a slight GC-bias for the insert sequences (see Figure S2e, S2f). Although
175 we did not find a predominant motif and hence this signature does not appear
176 to affect uniformity of coverage (see Figure S2g), it remains to be seen whether
177 or not future engineered Tn5 mutants can bypass this bias. In fact, a Tn5 mutant
178 showing reduced GC insertion bias on dsDNA has been reported previously
179 (21). In addition, the *in vitro* tagmentation efficiency of Tn5 on RNA/DNA hybrids

180 is low compared to its native substrate dsDNA. As wild-type Tn5 transposase
181 has been engineered to obtain hyperactive forms (4, 22-24), it is also tempting
182 to speculate that hyperactive mutants towards RNA/DNA hybrids could also be
183 obtained through screening and protein engineering. Such hyperactive mutants
184 are expected to have immediate utility in single-cell RNA-seq experiments, for
185 instance. Moreover, Tn5 transposition *in vivo* has been harnessed to profile
186 chromatin accessibility in ATAC-seq (10); it remains to be seen whether or not
187 an equivalent version may exist to enable *in vivo* detection of R-loop, chromatin
188 bound long non-coding RNA and epitranscriptome analysis (15, 16, 25). To
189 summarize, ATRAC-seq manifests a “cryptic” activity of the Tn5 transposase as
190 a powerful tool, which may have broad biomedical applications in the future.

191

192 **Materials and Methods**

193 **Cell culture**

194 HEK293T cells used in this study were daily maintained in DMEM medium
195 (GIBCO) supplemented with 10% FBS (GIBCO) and 1% penicillin/streptomycin
196 (GIBCO) at 37°C with 5% CO₂.

197

198 **RNA isolation**

199 Total RNA was extracted from cells with TRIzol (Invitrogen), according to the
200 manufacturer’s instructions. The resulting total RNA was treated with DNase I
201 (NEB) to avoid genomic DNA contamination. Phenol/chloroform extraction and

202 ethanol precipitation were then performed to purify and concentrate total RNA.

203 For mRNA isolation, two successive rounds of poly(A)⁺ selection were

204 performed using oligo(dT)₂₅ dynabeads (Invitrogen).

205

206 **Preparation of RNA/DNA hybrids**

207 Total RNA, mRNA and an *in vitro* transcribed model mRNA (IRF9) were reverse

208 transcribed into RNA/DNA hybrids by SuperScript IV reverse transcriptase

209 (Invitrogen), according to the manufacturer's protocol, with several

210 modifications: 1) Instead of oligo d(T)₂₀ primer, oligo d(T)₂₃VN primer (NEB) was

211 annealed to template RNA; 2) Instead of SS IV buffer, SS III buffer

212 supplemented with 7.5% PEG8000 was added to the reaction mixture; 3) The

213 reaction was incubated at 55°C for 2 h.

214

215 **Tn5 *in vitro* tagmentation on RNA/DNA hybrids**

216 Partial double-stranded adaptor A and B were obtained by separately annealing

217 10 μM primer A (5'-TCGTCGGCAGCGTCAGATGTGTATAAGAGACAG-3') and

218 primer B (5'-GTCTCGTGGGCTCGGAGATGTGTATAAGAGACAG-3') with

219 equal amounts of mosaic-end oligonucleotides (5'-CTGTCTCTTATACACATCT

220 -3'). Assembly of Tn5 with equimolar mixture of annealed Adaptor A and B was

221 performed according to the manufacturer's protocol (Vazyme). The resulting

222 assembled Tn5 was stored at -20°C until use.

223

224 Tagmentation reaction was set up by adding RT products, 12 ng/μl assembled
225 Tn5 and 1 U/μl SUPERase-In RNase Inhibitor (Invitrogen) to the reaction buffer
226 containing 10 mM Tris-HCl (pH = 7.5), 5 mM MgCl₂, 8% PEG8000. The reaction
227 was performed at 55°C for 30 min, and then SDS was added to a final
228 concentration of 0.04% and Tn5 was inactivated for 5 min at room temperature.

229

230 **Assays of tagmentation activity of Tn5 on RNA/DNA hybrids**

231 For testing tagmentation activity of Tn5 on RNA/DNA hybrids, reactions were
232 carried out as above, with 25ng mRNA derived RT products as substrate. The
233 tagmentation products were then purified using 1.8X Agencourt RNAClean XP
234 beads (Beckman Coulter) to remove Tn5 and excess free adaptors and eluted
235 in 6μl nuclease-free water. The size distribution of RNA/DNA hybrids after
236 tagmentation was assessed by a Fragment Analyzer Automated CE System
237 with DNF-474 High Sensitivity NGS Fragment Analysis Kit (AATI).

238

239 For testing tagmentation activity of Tn5 on RNA/DNA hybrids by quantitative
240 polymerase chain reaction (qPCR), tagmentation products purified as above
241 (100X-diluted) was firstly strand-extended with 0.32 U/μl Bst 3.0 DNA
242 Polymerase (NEB) and 1X AceQ Universal SYBR qPCR Master Mix (Vazyme)
243 at 72°C for 15 min, and then Bst 3.0 Polymerase was inactivated at 95°C for 5
244 min. After adding 0.2 μM qPCR primers (5'-AATGATACGGCGACCACCGAGA
245 TCTACTCGTCGGCAGCGTC-3'; 5'-CAAGCAGAAGACGGCATAACGAGAT

246 GTCTCGTGGGCTCGG-3'), qPCR was performed in a LightCycler (Roche)
247 with a 5 min pre-incubation at 95°C followed by 40 cycles of 10 sec at 95°C and
248 40 sec at 60°C. For testing the effect of different buffers on tagmentation activity
249 of Tn5 on RNA/DNA hybrids, buffers used were as follows: 1) Tagment buffer L
250 (Vazyme); 2) Buffer with 8% PEG8000 (10 mM Tris-HCl at pH 7.5, 5 mM MgCl₂,
251 8% PEG8000); 3) Buffer with 10% DMF (10 mM Tris-HCl at pH 7.5, 5 mM MgCl₂,
252 10% DMF).

253

254 **ATRAC-seq library preparation and sequencing**

255 For ATRAC-seq library preparation, all reactions were performed in one tube.
256 Reverse transcription and tagmentation reactions were carried out as above.
257 Strand extension reaction was performed by directly adding 0.32 U/μl Bst 3.0
258 DNA Polymerase and 1X NEBNext Q5 Hot Start HiFi PCR Master Mix (NEB)
259 to tagmentation products and incubating at 72°C for 15 min, followed by Bst 3.0
260 DNA Polymerase inactivation at 80°C for 20 min. Next, 0.2 μM indexed primers
261 were added to perform enrichment PCR as follows: 30 sec at 98°C, and then n
262 cycles of 10 sec at 98°C, 75 sec at 65°C, followed by the last 10min extension
263 at 65°C. The PCR cycles “n” depends on the amount of purified total RNA input
264 (200 ng, n = 15; 20 ng, n = 20; 2 ng, n = 25). After enrichment, the library was
265 purified twice using 1X Agencourt AMPure XP beads (Beckman Coulter) and
266 eluted in 10 μl nuclease-free water. The concentration of resulting libraries was
267 determined by Qubit 2.0 fluorometer with the Qubit dsDNA HS Assay kit

268 (Invitrogen) and the size distribution of libraries was assessed by a Fragment
269 Analyzer Automated CE System with DNF-474 High Sensitivity NGS Fragment
270 Analysis Kit. Finally, libraries were sequenced on the Illumina Hiseq X10
271 platform which generated 2 x 150 bp of paired-end raw reads.

272

273 **Data analysis**

274 Raw reads from sequencing were firstly subjected to Trim_galore (v0.6.4_dev)
275 (http://www.bioinformatics.babraham.ac.uk/projects/trim_galore/) for quality
276 control and adaptor trimming. The minimal threshold of quality was 20, and the
277 minimal length of reads to remain was set as 20 nt. Then trimmed reads were
278 mapped to human (hg19) genome and transcriptome using Tophat2 (v2.1.1)
279 (26), and the transcriptome was prepared based on the Refseq annotation of
280 human (hg19) downloaded from the table browser of UCSC database. rRNA
281 contamination were determined through directly mapping to the dataset of
282 human rRNA sequence downloaded from NCBI by bowtie2 (v2.2.9) (27).
283 Performances related to the processing of sam/bam file were done with the
284 help of Samtools (v1.9) (28). The FPKM, gene body coverage, reads
285 distribution, nucleotide composition for each position of read and GC content
286 distribution of mapped reads were calculated by RseqQC (v2.6.4) (29), and
287 insert size of library was calculated by Picard Tools (v2.20.6)
288 (<http://broadinstitute.github.io/picard/>). And all corresponding graphs were

289 plotted using R scripts. Reads Coverage was visualized using the IGV genome
290 browser (v2.4.16) (30).

291

292 **Acknowledgments**

293 The authors would like to thank Mr. Dongsheng Bai for discussions. We thank
294 National Center for Protein Sciences at Peking University in Beijing, China, for
295 assistance with evaluation of tagmentation efficiency and library size
296 distribution. This work was supported by the National Natural Science
297 Foundation of China (nos. 31861143026 and 91740112 to C.Y.), and Ministry
298 of Science and Technology of China (nos. 2019YFA0110900 and
299 2019YFA0802201 to C.Y.)

300

301 **Author Contributions**

302 B.L., C.Z. and C.Y. conceived the project; B.L., L.D., D.Y. and C.Y. designed the
303 experiments together and wrote the manuscript; B.L., L.D. and D.Y. performed
304 experiments with the help of M.Z. and X.L.; B.L. performed the bioinformatics
305 analysis with the help of C.Y. All authors commented on and approved the paper.

306

307 **Competing interests**

308 The authors declare no competing interests.

309

310 **Data Availability**

311 High-throughput sequence data has been deposited in Gene Expression

312 Omnibus (GEO) under accession code GSE143422.

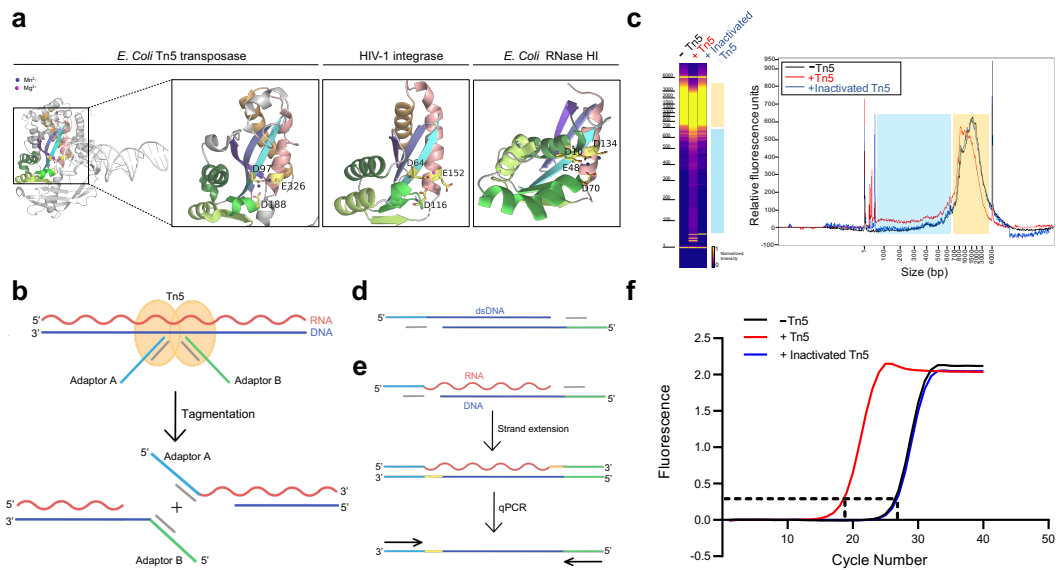
313

314 **References**

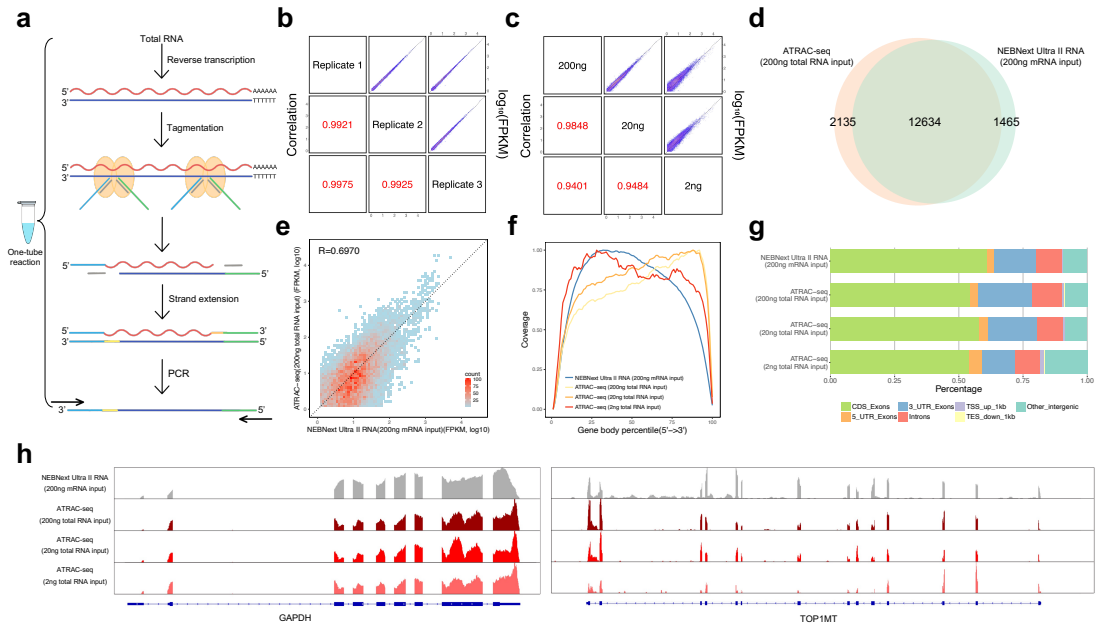
- 315 1. Kleckner N. Transposable elements in prokaryotes. *Annu Rev Genet.* 1981;15:341-404.
- 316 2. Finnegan DJ. Eukaryotic transposable elements and genome evolution. *Trends Genet.*
- 317 1989;5(4):103-7.
- 318 3. Curcio MJ, Derbyshire KM. The outs and ins of transposition: from mu to kangaroo. *Nat Rev*
- 319 *Mol Cell Biol.* 2003;4(11):865-77.
- 320 4. Goryshin IY, Reznikoff WS. Tn5 in vitro transposition. *J Biol Chem.* 1998;273(13):7367-74.
- 321 5. Adey A, Morrison HG, Asan, Xun X, Kitzman JO, Turner EH, et al. Rapid, low-input, low-bias
- 322 construction of shotgun fragment libraries by high-density in vitro transposition. *Genome Biol.*
- 323 2010;11(12):R119.
- 324 6. Picelli S, Bjorklund AK, Reinius B, Sagasser S, Winberg G, Sandberg R. Tn5 transposase and
- 325 tagmentation procedures for massively scaled sequencing projects. *Genome Res.*
- 326 2014;24(12):2033-40.
- 327 7. Caruccio N. Preparation of next-generation sequencing libraries using Nextera technology:
- 328 simultaneous DNA fragmentation and adaptor tagging by in vitro transposition. *Methods in*
- 329 *molecular biology.* 2011;733:241-55.
- 330 8. Ramskold D, Luo S, Wang YC, Li R, Deng Q, Faridani OR, et al. Full-length mRNA-Seq from
- 331 single-cell levels of RNA and individual circulating tumor cells. *Nat Biotechnol.* 2012;30(8):777-82.
- 332 9. Gertz J, Varley KE, Davis NS, Baas BJ, Goryshin IY, Vaidyanathan R, et al. Transposase mediated
- 333 construction of RNA-seq libraries. *Genome Res.* 2012;22(1):134-41.
- 334 10. Buenrostro JD, Giresi PG, Zaba LC, Chang HY, Greenleaf WJ. Transposition of native chromatin
- 335 for fast and sensitive epigenomic profiling of open chromatin, DNA-binding proteins and
- 336 nucleosome position. *Nature methods.* 2013;10(12):1213-8.
- 337 11. Yang W, Steitz TA. Recombining the structures of HIV integrase, RuvC and RNase H. *Structure.*
- 338 1995;3(2):131-4.
- 339 12. Savilahti H, Rice PA, Mizuuchi K. The phage Mu transpososome core: DNA requirements for
- 340 assembly and function. *EMBO J.* 1995;14(19):4893-903.
- 341 13. Nowotny M. Retroviral integrase superfamily: the structural perspective. *EMBO Rep.*
- 342 2009;10(2):144-51.
- 343 14. Rice PA, Baker TA. Comparative architecture of transposase and integrase complexes. *Nat*
- 344 *Struct Biol.* 2001;8(4):302-7.
- 345 15. Santos-Pereira JM, Aguilera A. R loops: new modulators of genome dynamics and function.
- 346 *Nat Rev Genet.* 2015;16(10):583-97.
- 347 16. Li X, Fu XD. Chromatin-associated RNAs as facilitators of functional genomic interactions. *Nat*
- 348 *Rev Genet.* 2019;20(9):503-19.
- 349 17. Nowotny M, Gaidamakov SA, Crouch RJ, Yang W. Crystal structures of RNase H bound to an
- 350 RNA/DNA hybrid: substrate specificity and metal-dependent catalysis. *Cell.* 2005;121(7):1005-16.

- 351 18. Goryshin IY, Miller JA, Kil YV, Lanzov VA, Reznikoff WS. Tn5/IS50 target recognition.
352 Proceedings of the National Academy of Sciences of the United States of America.
353 1998;95(18):10716-21.
- 354 19. Green B, Bouchier C, Fairhead C, Craig NL, Cormack BP. Insertion site preference of Mu, Tn5,
355 and Tn7 transposons. *Mob DNA*. 2012;3(1):3.
- 356 20. Lodge JK, Weston-Hafer K, Berg DE. Transposon Tn5 target specificity: preference for
357 insertion at G/C pairs. *Genetics*. 1988;120(3):645-50.
- 358 21. Kia A, Gloeckner C, Osothpraprop T, Gormley N, Bomati E, Stephenson M, et al. Improved
359 genome sequencing using an engineered transposase. *BMC Biotechnology*. 2017;17(1):6.
- 360 22. Wiegand TW, Reznikoff WS. Characterization of two hypertransposing Tn5 mutants. *J*
361 *Bacteriol*. 1992;174(4):1229-39.
- 362 23. Weinreich MD, Gasch A, Reznikoff WS. Evidence that the cis preference of the Tn5
363 transposase is caused by nonproductive multimerization. *Genes Dev*. 1994;8(19):2363-74.
- 364 24. Zhou M, Reznikoff WS. Tn5 transposase mutants that alter DNA binding specificity. *J Mol Biol*.
365 1997;271(3):362-73.
- 366 25. Li X, Xiong X, Yi C. Epitranscriptome sequencing technologies: decoding RNA modifications.
367 *Nature methods*. 2016;14(1):23-31.
- 368 26. Kim D, Pertea G, Trapnell C, Pimentel H, Kelley R, Salzberg SL. TopHat2: accurate alignment
369 of transcriptomes in the presence of insertions, deletions and gene fusions. *Genome Biology*.
370 2013;14(4):R36.
- 371 27. Langmead B, Salzberg SL. Fast gapped-read alignment with Bowtie 2. *Nat Methods*.
372 2012;9(4):357-9.
- 373 28. Li H, Handsaker B, Wysoker A, Fennell T, Ruan J, Homer N, et al. The Sequence
374 Alignment/Map format and SAMtools. *Bioinformatics*. 2009;25(16):2078-9.
- 375 29. Wang L, Wang S, Li W. RSeQC: quality control of RNA-seq experiments. *Bioinformatics*.
376 2012;28(16):2184-5.
- 377 30. Robinson JT, Thorvaldsdóttir H, Winckler W, Guttman M, Lander ES, Getz G, et al. Integrative
378 genomics viewer. *Nature biotechnology*. 2011;29(1):24-6.

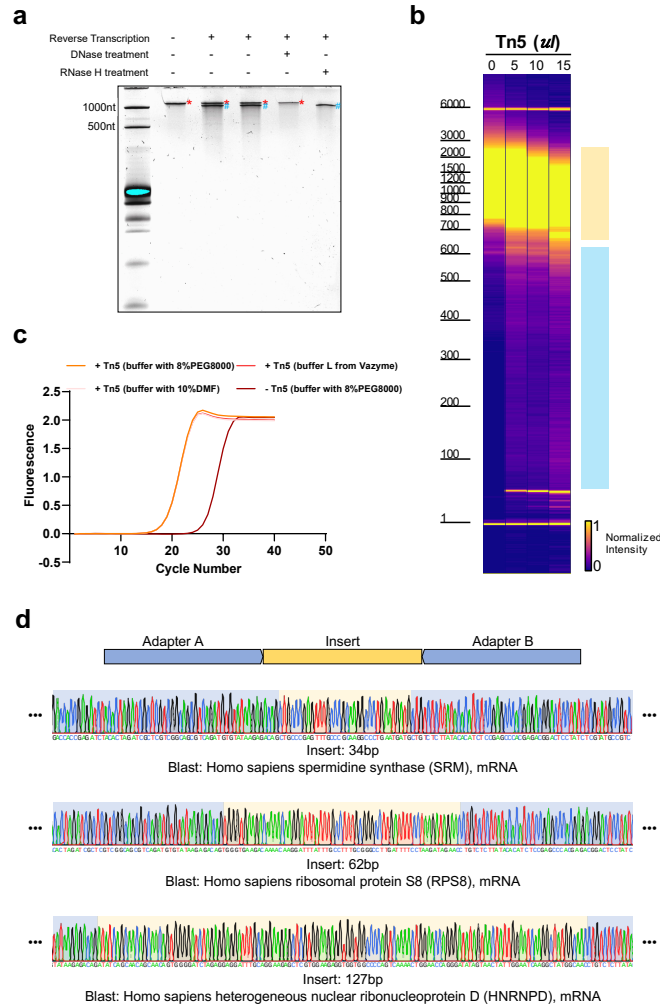
379



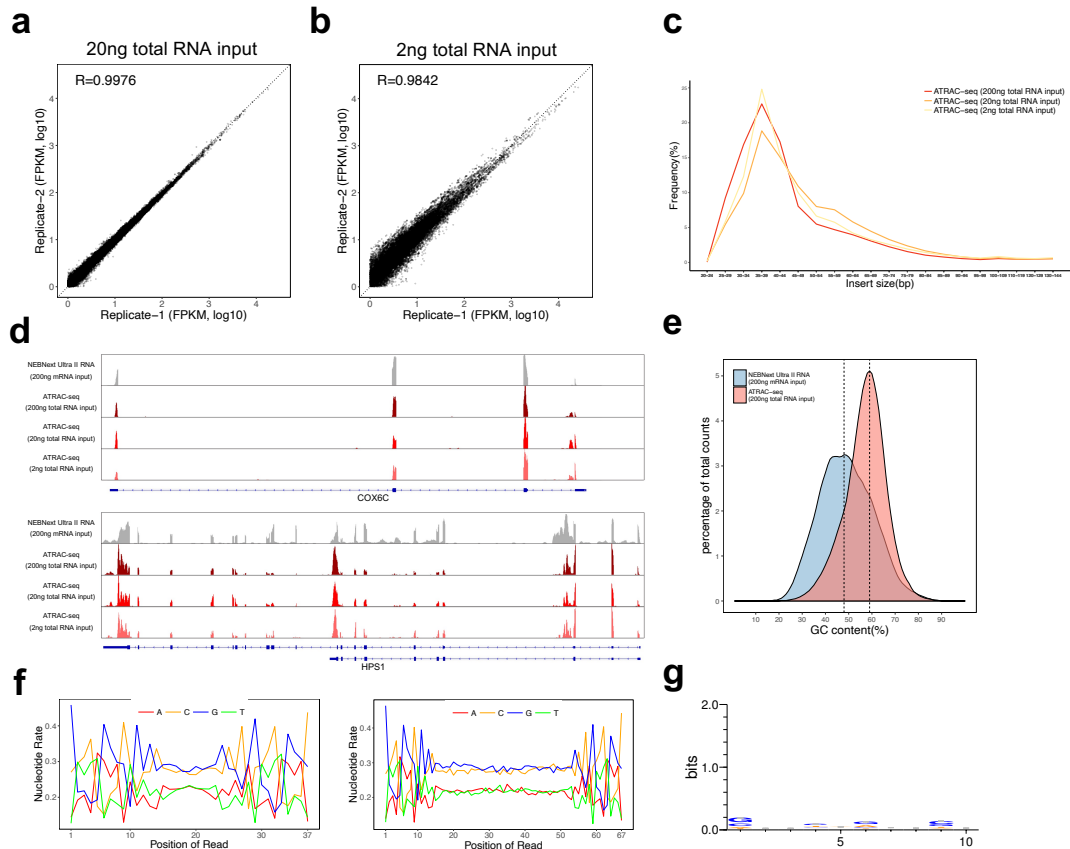
380 **Figure 1.** Tn5 transposome has direct tagmentation activity on RNA/DNA hybrid duplexes. **(a)** Crystal
 381 structure of a single subunit of *E. coli* Tn5 Transposase (PDB code 1MM8) complexed with ME DNA
 382 duplex, and zoom-in views of the conserved catalytic core of Tn5 transposase, HIV-1 integrase (PDB code
 383 1BIU), and *E. coli* RNase HI (PDB code 1G15), all of which are from the retroviral integrase superfamily.
 384 Active-site residues are shown as sticks, and the Mn^{2+} and Mg^{2+} ions are shown as deep blue and
 385 magenta spheres. **(b)** Schematic of Tn5-assisted tagmentation of RNA/DNA hybrids. **(c)** Gel pictures (left)
 386 and peak pictures (right) represent size distributions of RNA/DNA hybrid fragments after incubation
 387 without Tn5 transposome, with Tn5 transposome, and with inactivated Tn5 transposome. The blue and
 388 orange patches denote small and large fragments, respectively. **(d)** Schematic of the product of *in vitro*
 389 tagmentation reaction of the canonical dsDNA substrate. **(e)** Workflow of conversion of tagged RNA/DNA
 390 hybrids into amplifiable DNA sequences. **(f)** qPCR amplification curve of tagmentation products of
 391 samples with Tn5 treatment, with inactivated Tn5 treatment, or without Tn5 treatment. Average Ct values
 392 of two technical replicates are 18.06, 26.25 and 26.41, respectively.



393 **Figure 2.** Workflow and evaluation of ATRAC-seq. **(a)** Workflow of ATRAC-seq. **(b)** Gene expression, measured by three technical replicates of ATRAC-seq with 200 ng total RNA as input, are shown as scatter plots in the upper right half. Pearson's product-moment correlations are displayed in the lower left half. **(c)** Gene expression, measured by ATRAC-seq using 200 ng, 20 ng and 2 ng total RNA as input, are shown as scatter plots in the upper right half. Pearson's product-moment correlations are displayed in the lower left half. **(d)** Venn Diagram of gene numbers detected by ATRAC-seq with 200 ng total RNA as input and NEBNext Ultra II RNA kit with 200 ng mRNA as input. **(e)** Scatterplot showing gene expression values for ATRAC-seq with 200 ng total RNA as input and NEBNext Ultra II RNA kit with 200 ng mRNA as input. Pearson's product-moment correlation is displayed in the upper left corner. **(f)** Comparison of read coverage over gene body for ATRAC-seq with 200 ng, 20 ng and 2 ng total RNA as input and NEBNext Ultra II RNA kit with 200 ng mRNA as input. The read coverage over gene body is displayed along with gene body percentile from 5' to 3' end. **(g)** Comparison of the distribution of reads across known gene features for ATRAC-seq with 200 ng, 20 ng and 2 ng total RNA as input and NEBNext Ultra II RNA kit with 200 ng mRNA as input. **(h)** IGV tracks showing the coverage of two representative transcripts (GAPDH and TOP1MT). The data come from NEBNext Ultra II RNA kit and three sets of ATRAC-seq with different amount of total RNA.



409 **Figure S1.** Tagmentation activity of Tn5 transposome on RNA/DNA hybrids. **(a)** Denaturing (8 M urea)
 410 polyacrylamide gel analysis of reverse transcription products of an *in vitro* transcribed mRNA (IRF9). Lane
 411 1: ssRNA marker. Lane 2: *in vitro* transcribed mRNA (IRF9). Lane 3&4: reverse transcription products of
 412 an *in vitro* transcribed mRNA (IRF9). Lane 5: reverse transcription product treated with DNase I. Lane 6:
 413 reverse transcription product treated with RNase H. ssRNA and ssDNA is marked with a red asterisk and
 414 a blue pound sign, respectively. **(b)** Gel picture showing size distribution of RNA/DNA hybrids products of
 415 50 µl reaction systems without Tn5 transposome, and with 5 µl, 10 µl, and 15 µl Tn5 transposome,
 416 respectively. The blue and orange patches denote small and large fragments, respectively. **(c)** qPCR
 417 amplification curve of tagmentation products without Tn5 treatment or with Tn5 treatment in three different
 418 buffers (see methods). Average Ct values are 26.41, 18.39, 18.33 and 18.34, respectively. **(d)** Sanger
 419 sequencing chromatograms of PCR products following RNA/DNA hybrid tagmentation and strand
 420 extension. Adaptor A and B sequences are highlighted with blue background color and insert sequences
 421 are highlighted with yellow background.



422 **Figure S2.** Quality assessment of ATRAC-seq. **(a)** Gene expression measured by two technical replicates
 423 of ATRAC-seq with 20 ng total RNA as input are shown as scatter plots. Pearson's product-moment
 424 correlations are displayed in the upper left corner. **(b)** Gene expression measured by two technical
 425 replicates of ATRAC-seq with 2 ng total RNA as input are shown as scatter plots. Pearson's product-
 426 moment correlations are displayed in the upper left corner. **(c)** Distribution of the insert size in ATRAC-
 427 seq data with 200 ng, 20 ng and 2 ng total RNA as input, respectively. **(d)** IGV tracks displaying the
 428 coverage of representative transcripts of a highly expressed gene COX6C, and a moderately expressed
 429 gene HPS1. **(e)** Distribution of GC content of all mapped reads from ATRAC-seq library with 200 ng total
 430 RNA as input and NEBNext Ultra II RNA library with 200 ng mRNA as input. Two vertical dashed lines
 431 indicate 48% and 59%. **(f)** Nucleotide versus cycle (NVC) plots showing percentage of observed bases
 432 at each position of mapped 37bp and 67bp reads from ATRAC-seq library with 200 ng total RNA as input.
 433 **(g)** Per-position information content of Tn5 insertion sites on RNA/DNA hybrids.

Library type	Mapping rate	rRNA rate	Genes
NEBNext Ultra II RNA (200ng mRNA input) replicate 1	84.4%	4.3%	14099
NEBNext Ultra II RNA (200ng mRNA input) replicate 2	83.4%	4.7%	14072
ATRAC-seq (200ng total RNA input) replicate 1	87.9%	9.8%	14769
ATRAC-seq (200ng total RNA input) replicate 2	87.3%	8.7%	14713
ATRAC-seq (20ng total RNA input) replicate 1	89.3%	5.5%	14899
ATRAC-seq (20ng total RNA input) replicate 2	87.9%	9.7%	14964
ATRAC-seq (2ng total RNA input) replicate 1	69.5%	20.6%	13532
ATRAC-seq (2ng total RNA input) replicate 2	69.1%	17.8%	14213

434 **Table S1.** Quality control of the sequencing results using NEBNext kit and ATRAC-seq.